

Measuring Negative Inductance

OELP Final Report

by

Manikantan R S

(122101046)

Kevin R Jacob

(122101018)

under the guidance of

Dr. Arvind Ajoy



**INDIAN INSTITUTE
OF TECHNOLOGY
PALAKKAD**

to the

DEPARTMENT OF ELECTRICAL ENGINEERING

INDIAN INSTITUTE OF TECHNOLOGY PALAKKAD

Abstract

In recent years, negative capacitance has risen in popularity with its effect manifesting in ferro-electric materials and its promise of paving a way to create more energy efficient electronics. This prompts the question of existence of a dual, which is negative inductance (NI). As seen in simulations and convincingly in experiment, this manifests as a momentous drop in current with increase in flux, or momentous rise in current with decrease in flux, for which this phenomenon can be appropriately named as “transient negative inductance”. This work effectively captures the behaviour of a ferromagnetic (FM) inductor in transient when it changes in polarization.

Contents

1	Introduction	3
2	Modeling Ferromagnetic system	4
2.1	Landau Theory Model	4
2.2	Ising Model	5
3	Simulation Results	8
4	Experimental Validation	10
4.1	Core Characterization- Hysteresis Measurements	10
4.2	Measuring Negative Inductance - Experimental setup	11
5	Current Source	12
5.1	Theory	12
5.2	Simulation	13
5.3	Breadboard testing	14
5.3.1	PCB design - Schematic	15

5.3.2	PCB design - Layout	17
5.4	PCB printing and Assembling	18
5.5	Testing - Results	19
6	Automating Test-setup	20
6.1	Py-Visa	20
7	Experiment Results	21
7.1	Hysteresis	21
7.2	Negative Inductance	22
7.2.1	Results Obtained Using Source-Meter-Unit	22
7.2.2	Results From the V-I converter	22
8	Conclusion	26
8.1	Comprehending Simulation and Measurement Results	26
8.2	Comparison With the Negative Capacitance Results	26

1 Introduction

Negative Inductance can be understand as a transient phenomenon. Inductance is change in current per change in flux ($L = \frac{di}{d\phi}$), therefore negative inductance means the current is increasing while the flux is decreasing or the when the current is decreasing the flux is increasing. This phenomenon is theoretically explained by Landau theory, which models the ferromagnet as a double well system, and the transient negative inductance is observed when the system transfer via the unstable minima of the double well. Despite of the theoretical existence of phenomenon, no research work has yet shown it in measurements ([2] a paper which talks about "Nonlinear Dynamical Circuit Analysis of a Ferromagnetic Inductor" has some similar results but, the discussion is in different contest). There are multiple reasons since the ferromagnetic core available are pure multi-domain system with significant amount of crystal defects, therefore the Landau theory barely holds. The need of much more accurate model is essential for the justification of our research. Ising model, a stochastic dual spin model is well known approximation of ferromagnets, this model is usually employed in simulations involving phase transition with respect to temperature. With this model and a robust test setup, we are investigating the existence of transient negative inductance.

This OELP is the continuation of a BTP project by Priyankka G. R. (121801039) under the guidance of Dr. Arvind Ajoy [3], and continuation from our Previous semester OELP work. (More emphasise has given to the work done on this semester, Previous works are mentioned for maintaining the continuity of the report).

2 Modeling Ferromagnetic system

The Landau based single domain model and the Ising based multi-domain model both showcase the qualitative behaviour of a negative inductor. Single-domain ferromagnetic materials display a double-well behavior in their energy versus flux plot, as described by the Landau equation. The existences of negative inductance is theoretically explained by the Landau equation. However, real-world ferromagnetic cores are typically multi-domain systems. To capture the qualitative behavior of ferromagnetic cores when subjected to a switching magnetic field, a 3D Ising model is employed. The solution to the Ising model is obtained using the Monte Carlo algorithm.

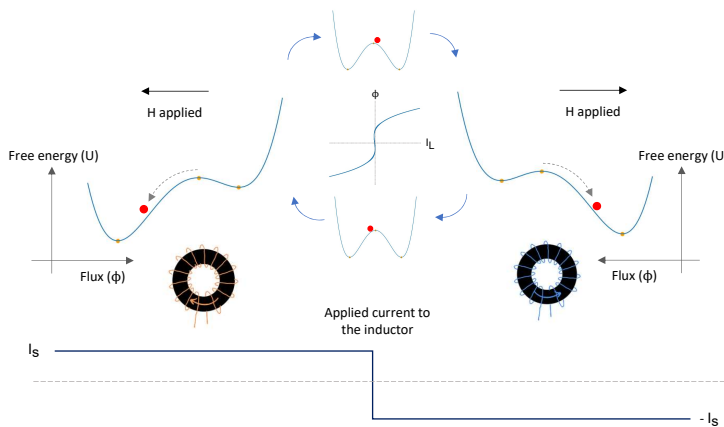


Figure 1: Transient in Multi-domain Ferromagnet

2.1 Landau Theory Model

In Landau based model, ferromagnets are bistable single domain system with a double well energy landscape, with two stable states representing spin up and spin down states of FM. The energy-flux relation is described by equation.

$$U = \alpha\phi^2 + \beta\phi^2 - \phi I_L \quad (1)$$

For the time-dependent switching on magnetic field, Landau-Ginzburg equation is used.

$$\rho \frac{d\phi}{dt} = -\frac{dU}{d\phi} \quad (2)$$

To see the transient NI effect clearly, square current waveform is used to excite the inductor. A low resistance is added to slow down the transient period. The results obtained are shown in Figure. The S curve corresponds to the transient NI switching hysteresis.

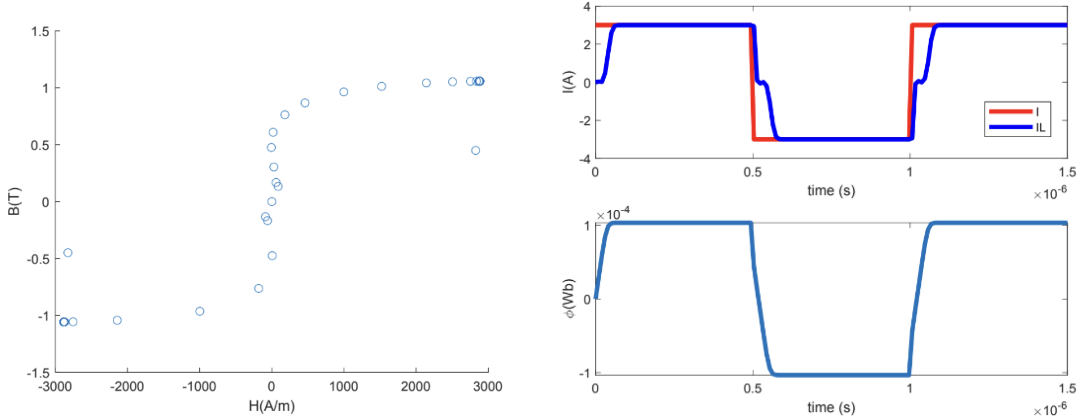


Figure 2: Landau theory simulation

2.2 Ising Model

Ising model is a multi-domain model for ferromagnetic materials which consider each dipole in the FM to be an individual entity. It is commonly used to show phase transition with respect to temperature, for this study we adapt this model to show the hysteresis and transient negative inductance behaviour. A 3D Ising model with circular boundary condition is used to simulate the toroid used in the work. Transient negative inductance is observed in the simulation results of the qualitative model in the multidomain FM.

The Hamiltonian of the system is given by :

$$\hat{H} = \sum_i \sum_{\langle ij \rangle} J_{i,j} \sigma_i \sigma_j + \sum_i H \sigma_i \quad (3)$$

where $J_{i,j}$ quantify the interaction energy between nearest neighbours. second term quantify the energy corresponding to an external H.

The energy change in the system due to the switching of a single dipole is given by (from +1 to -1, or from -1 to +1)

$$d\hat{H} = 2 \sum_{\langle ij \rangle} J_{i,j} \sigma_i \sigma_j + 2H \sigma_i \quad (4)$$

The system retain the flip of dipole if the change in energy is negative, leading to a more stable system. Else flip is retained with a probability determined by Boltzmann distribution

$$P = \exp \frac{-d\hat{H}}{k_b T} \quad (5)$$

for the simulation we consider a normalized system of values and make $k_b = 1$, the effective magnetic field to be H/H_c . For solving the model monte-carlo approach is adopted, random spin choosing and switching happens multiple times per second determined by the switching speed of the system. The total magnetization of the system is calculated as:

$$M = \frac{1}{N_x.N_y.N_z} \sum_{\langle i,j,k \rangle} \sigma_{ijk} \quad (6)$$

the normalized results (H and M) are then multiplied with the scaling factors (H_c and M_c) obtained from the experiment results to get the actual values of Magnetization and magnetic field.

Algorithm 1: Ising Model - Monte-Carlo

Initialization of **Parameters**;

I = create a square current waveform from +Io to -Io with dt and frequncy f (n points) ;

initialize the lattice spin values (list[Nx][Ny][Nz]) with +1 or -1;

for $i = 1$ **to** n **do**

 assign a guess value for inductor current (IL) ;

while *True* **do**

 compute $H = \frac{N \cdot IL}{L_c}$;

for $j = 1$ **to** *suspeed * dt* **do**

 (x,y,z) = random lattice position;

 flip the spin value at (x,y,z);

 compute $d\hat{H} = 2 \sum_{<ij>} J_{i,j} \sigma_i \sigma_j + 2H \sigma_i$;

 retain the spin if the dH is negative else with a probability of $\exp \frac{-d\hat{H}}{k_b T}$;

 compute $M = \frac{1}{N_x \cdot N_y \cdot N_z} \sum_{<i,j,k>} \sigma_{ijk}$;

 compute $B = \mu(H + M)$;

 compute $\phi = B * A$;

 compute $I_R = \frac{d\phi}{dt * R}$;

 IL2 = I - IR;

if $IL2 == IL$ **then**

 break;

else

 IL = IL2;

 continue;

return IL, ϕ ;

Parameters	Description	Values	Quantity/Units
N_x, N_y, N_z	Domain size	25,25,70	unitless
$K_b T$	Temperature Energy	0.2	Energy (J or eV)
J	Interaction Coefficient	0.5	Energy (eV)
H_c	Scaling factor of H	1000	Energy (eV)
M_c	Scaling factor of M	10^5	scaling factor of M
Time	Total simulation time	0.5×10^{-4}	time (s)
dt	Sampling interval	0.2×10^{-6}	time (s)
swspeed	No: switches in one second	10^7	frequency of switches (unitless)

Table 1: Ising Model Parameters

3 Simulation Results

The simulation is performed with multiple set of parameter values, studying the result of effect of each parameter in the simulation results. By tweaking the values of the dt and $sfspeed$ the convergence of the M_c is ensured. H_c and M_c are obtained by matching the hysteresis graph with the actual datasheet values.

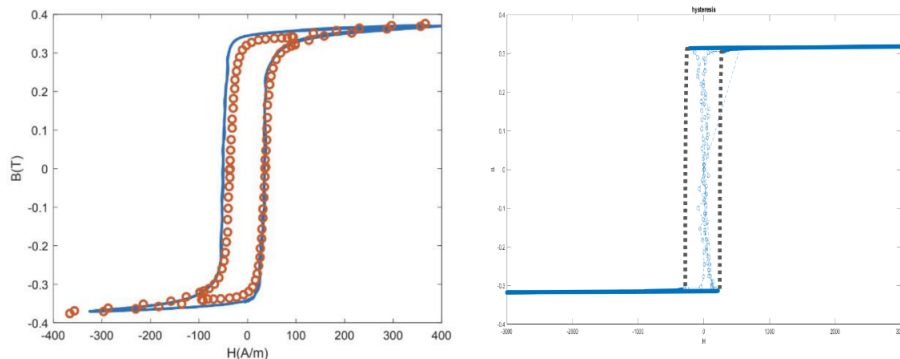


Figure 3: The value of H_c and M_c used in the simulations are fixed by fitting the hysteresis obtained from the Ising model simulations to the hysteresis of the core

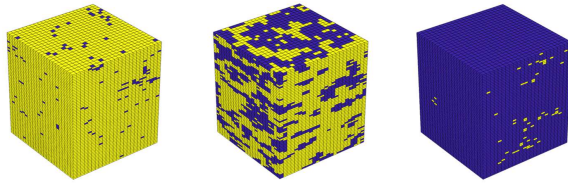


Figure 4: The spin switching while H is reversed (yellow and blue are two opposite spins)

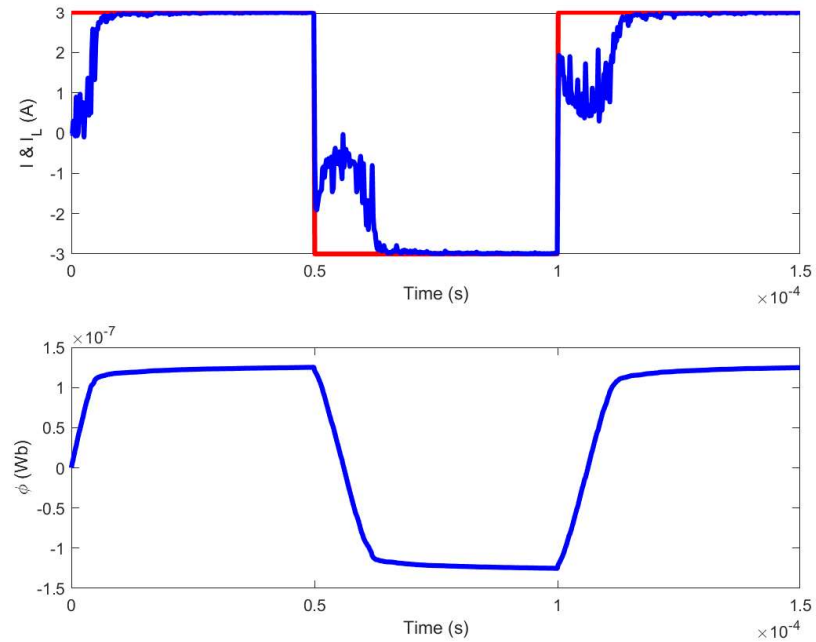


Figure 5: Result showing transient negative inductance

The value of J self interaction energy term is not known.

Also the results obtained only show the behaviour of such a system since the model is not able to account any actual physical values.

The convergence property of the solver is not great. It is diverging for a lot set of parameter values, also the simulation time is also significantly higher.

Parameters	Description	Values	Quantity/Units
L_c	Effective inductor length	0.01	length (m)
A	Effective cross sectional area	10^{-6}	area (m^2)
Nut	no: turns	10	unitless
R	Parallel Resistance (for reducing transient time)	10^{-2}	Resistance (Ω)

Table 2: Experiment setup Modeling Parameters

4 Experimental Validation

4.1 Core Characterization- Hysteresis Measurements

Understanding the characteristics of the ferromagnetic core is essential for comparison of the results with the Simulation Models and it is essential to know what is the saturation flux for the core.

The hysteresis set up consists of a voltage follower with power transistor based enhanced current capability. The circuit can be seen in the Figure 6.

The current and voltage across the inductor are measured through the voltage points.

$$B = \frac{1}{NA} \int V_L dt \quad (7)$$

$$H = \frac{NI_L}{l} \quad (8)$$

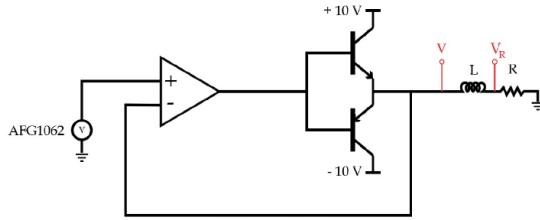


Figure 6: Experiment Setup for measuring Hysteresis

From these equations, the core hysteresis can be obtained.

4.2 Measuring Negative Inductance - Experimental setup

The experimental setup to measure transient negative inductance includes a square wave current source driving a ferromagnetic toroid inductor in parallel with a small resistance, analogous to the experiment performed by Dr.Asif Khan and team[1] to measure negative capacitance (A square wave voltage source driving a ferro-electric capacitor and large resistance in series. For realizing this experimental setup we need a current source that can supply upto 2A current at a voltage rating of atleast 7 to 8 V. For testing out this analogy setup, Source Meter Unit (SMU) is used, SMU can be programmed to behave like a current source, but the operating frequency (max 100 Hz) and transient time (around 1 ms) when switching from source to sink current are not ideal.

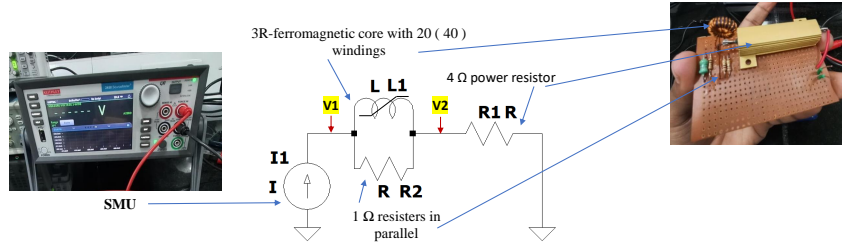


Figure 7: Experiment Setup with the SMU

The results obtained from this setup is discussed is the result section. since Therefore the need for a fast switching ideal current source for this test setup is i

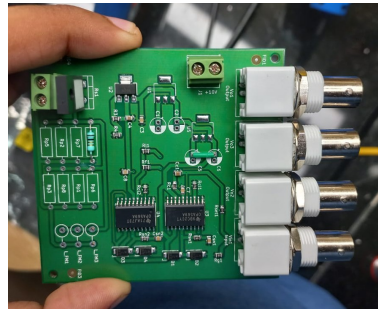


Figure 8: Experiment Setup with the V-I converter

5 Current Source

A square current waveform is needed for the measurement, a voltage to current converter appears to be the most suitable choice. The criteria include the capability of the current source to both source and sink current, with a power rating of at least 10 W, and a high slew rate. The circuit is realised using the opamp OPA569 a low-cost, high-current operational amplifier designed for driving various loads while operating on low-voltage supplies. OPA569 features a current monitoring pin that generates an output equal to 1/475th of the IC's output current. Utilizing this monitoring pin as feedback to the opamp enables the opamp's output current to mirror the supply voltage waveform, forming the fundamental concept behind the current source design. A design from TI utilizing two of these opamps in a floating load configuration was adopted, with modifications made to meet specific requirements, such as incorporating slots in the PCB for the measurement setup and routing connections through BNC cables.

5.1 Theory

From the design paper [4] This bridge-tied load (BTL) voltage-to-current (V-I) converter circuit creates a bidirectional current source used to drive a floating load from a single-ended source. The circuit makes use of an internal output current monitor circuit (IMON) in a specialty power amplifier. The V-I transfer function is accomplished by using the IMON current as the feedback for the first amplifier. The second amplifier inverts the output of the first amp to achieve the BTL operation which doubles the voltage swing and slew rate across the load, and allows for a bidirectional output from a single-ended power supply.

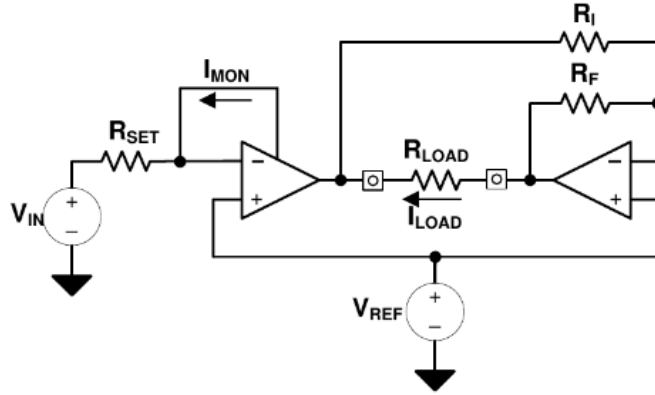


Figure 9: The schematic of the floating current source (V-I converter)

Transfer Function of the design:

$$I_{in} = \frac{V_{in}}{R_{set}} \quad (9)$$

$$I_{mon} = \frac{I_{out}}{475} \quad (10)$$

$$\therefore I_{Load} = \frac{V_{in} - V_{ref}}{R_{set}} \times 475 \quad (11)$$

5.2 Simulation

For simulating TINA-spice simulator is used. (TI's circuit simulator, since the spice model is not available on Ltspace)

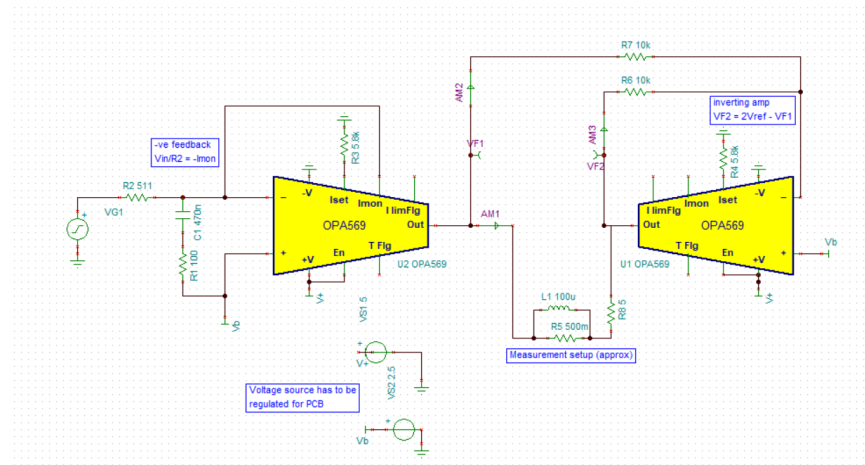


Figure 10: The simulation model



(a) Tested with a square voltage source of peak to peak 1V

(b) Switching from sinking to sourcing

Figure 11: Simulation Results

A step current source of approx. 100 Hz frequency with switching time approx. $10\mu s$ is required for the experiment the simulated results are given above, the input voltage with $10\mu s$ delay is feed to the circuit output has a switching time of approx. $15\mu s$

5.3 Breadboard testing

First the circuit is tested on breadboard for verifying the functionality. SOIC to DIP 20 pin adaptor is used to connect the SMD IC to breadboard, for breadboard testing all the voltage regulator, bypass capacitors, protection diodes, loop compensate filter are avoided.

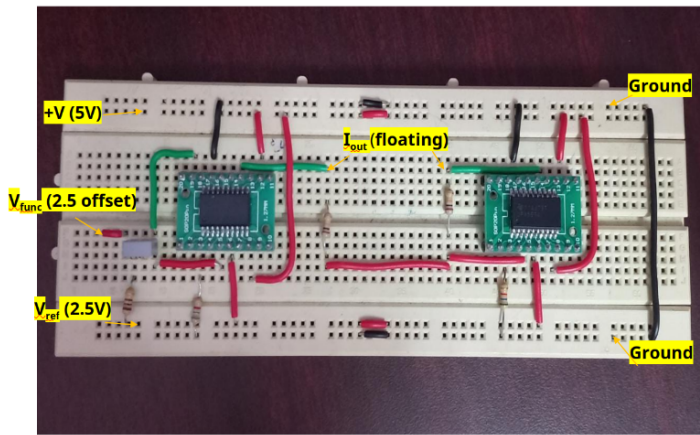


Figure 12: The setup tried on breadboard

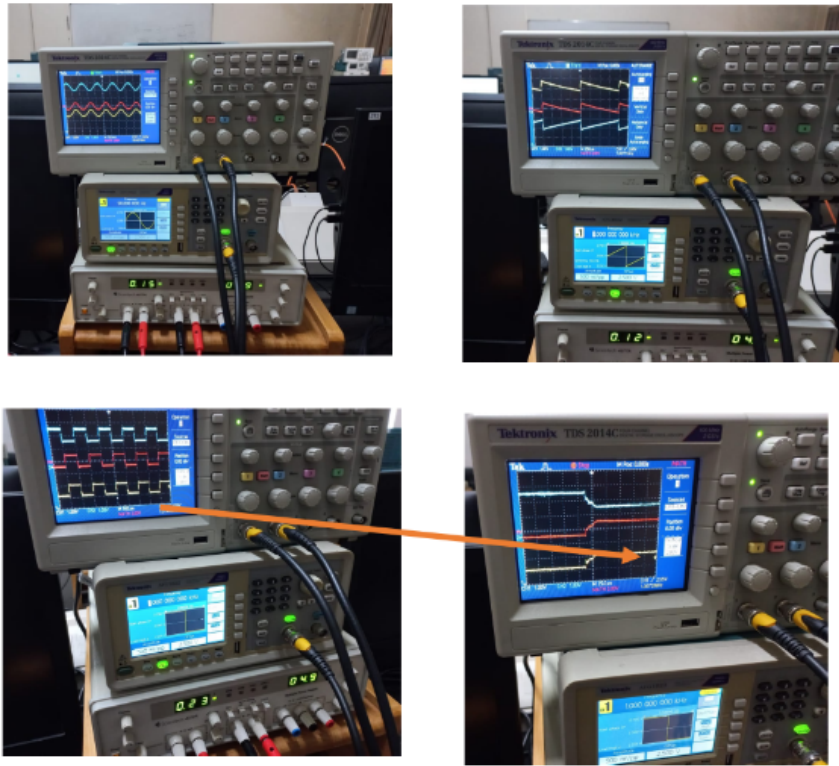


Figure 13: The output waveform obtained

4.2ohm power resistor were used to test the current source with different functions of voltage with 1kHz frequency. The setup is able to track the voltage to the output current. But this setup got damaged after some tries.

5.3.1 PCB design - Schematic

Voltage regulator LM7805 (5V regulotor) used for giving supply to opamps. LM317 is used to set the reference voltage to 2.5 V. Additional slots are added for the test-bench setup. All the measurement points are connected to the BNC connector output, the input voltage waveform also taken from a BNC connector. There is one additional pitch screw terminal added to get the current output from the setup to get the current output.

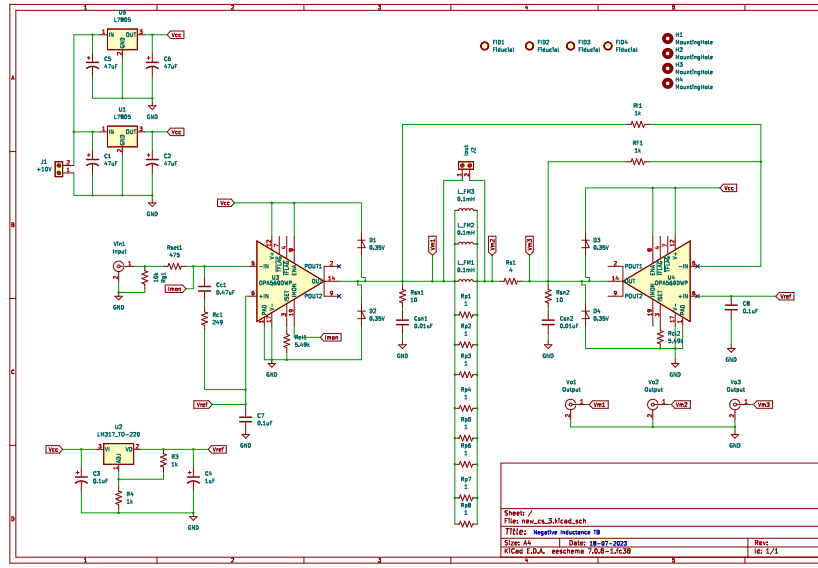


Figure 14: schematic diagram

Operational amplifier

To enable the V-I transfer function described in this design, the power amplifier needs to include an internal output current monitor, eliminating most power amplifier options. The OPA569 power amplifier is a high-current device that is capable of driving a wide variety of loads with an output current over 2 A. It is optimized for low-voltage, single or dual-supply operation with rail-to-rail swing on both the input and output.

Voltage reference

A +2.5 V reference voltage was applied to this circuit to accommodate for a bi-directional output with a single-supply. voltage regulator LM317 used for setting the reference voltage to 2.5 V, by setting the feedback resistor values in the same value (1K each). BNC connectors are used for input of voltage signal and take output from the measuring point as indicated in the schematic.

Output protection diode

Reactive and other electromotive force (EMF) generating loads can cause the output voltage to exceed the supply voltage, VCC, and potentially damage the circuit. This scenario can be avoided by clamping the output terminal voltage to the power supplies through the use of Schottky rectifier diodes. We used Schottky Rectifier, 45 V, 3 A, Single, DO-221AC, 2 Pins, 540 mV

Output Snubber Network (RSN, CSN)

Snubbers are frequently used in electrical systems with an inductive load where the sudden interruption of current flow leads to a large counter-electromotive force: a rise in voltage across the current switching device that opposes the change in current, in accordance with Faraday's law. With $R = 10 \Omega$ and $C = 0.01 \mu F$.

Loop Compensation Components (RC, CC)

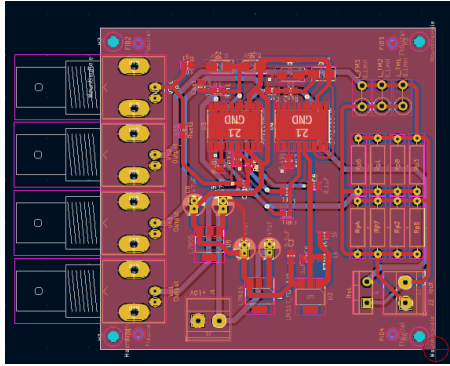
Compensation components RC and CC provide a high frequency path for currents to flow to the reference voltage at the non-inverting input. These components help dampen the response. The values are used directly from the design.

BNC connectors

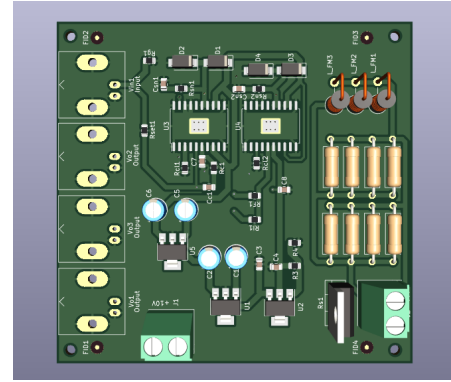
BNC connectors are used to take output measuring points from the circuit, the input voltage is also connected through a BNC connectors.

5.3.2 PCB design - Layout

The board dimension is $77mm \times 80mm$. Double sided PCB. Track width used for current path are 1mm. All expect the connectors and $47\mu F$ capacitors are SMD components



(a) PCB layout

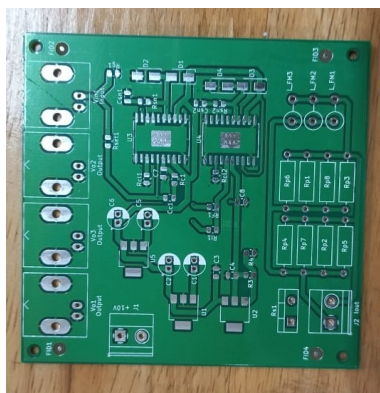


(b) PCB 3D view

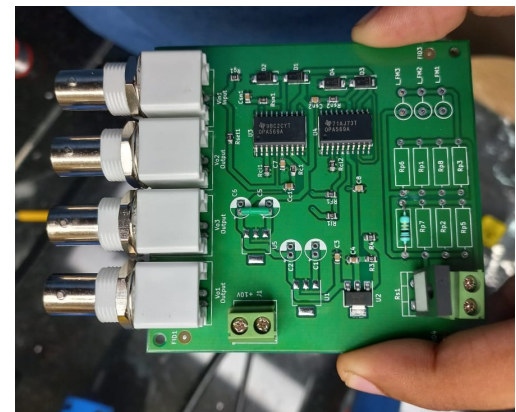
Figure 15: Layout

5.4 PCB printing and Assembling

PCB get printed from the Lioncircuits. Total cost for printing was around 3k rupees (including shipping charge), for 10 PCB (minimum order quantity). The PCB stencil is printed using laser-cutter. PCB assembling is done using Pick-and-Place machine from innovation lab, and re-flow oven is used for soldering. Rest of the components are hand soldered to the PCB.



(a) PCB before populating



(b) PCB

Figure 16: PCB

5.5 Testing - Results

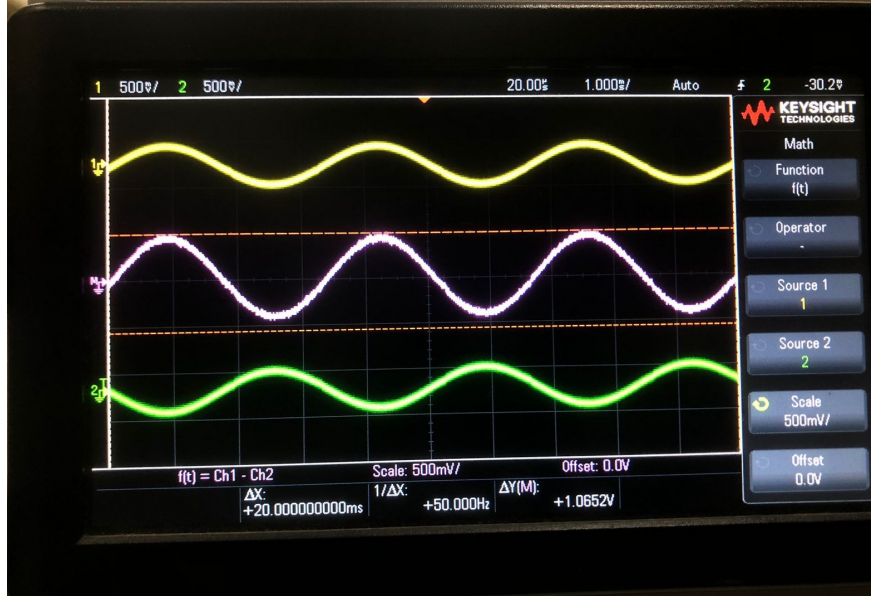


Figure 17: PCB tested in lab (violet line is the current waveform)



Figure 18: The response when the current source change from source to sink

The switching time is close to $15\mu s$ which is much better than SMU's response which was close to 1ms. The source is tried upto 1A it is working fine.

6 Automating Test-setup

Since a battery of tests had to conducted on the one setup which involved lots of data acquisition alongside simultaneous processing, a time and energy saving measure was to automate the data acquisition using python and other scripting activities.

6.1 Py-Visa

The Virtual Instrument Software Architecture or VISA is an application programming interface used in the test and measurement (T&M) industry for communicating with instruments from a computer. The python implementation of this is packed in the Pyvisa Module. Using the API, it is possible the control the instruments to control the test instruments as well as transfer waveform data directly without the need of an intermediate device.

Scripts were written to set a particular test condition¹ on the Signal Generator, then scale and acquire the raw data on the oscilloscope directly to the computer which can be processed better.

A programming guide is usually provided with the test instrument which serves as a reference for the scripting.

¹Set the frequency, Amplitude etc.

7 Experiment Results

7.1 Hysteresis

Here, the hysteresis plot has been done for multiple frequencies as it can be seen in Figure 20.

A single one of the data sets is shown in Figure 19 at frequency 1500.

The number of turns on the coil is 65 and the series resistance used is 10Ω .

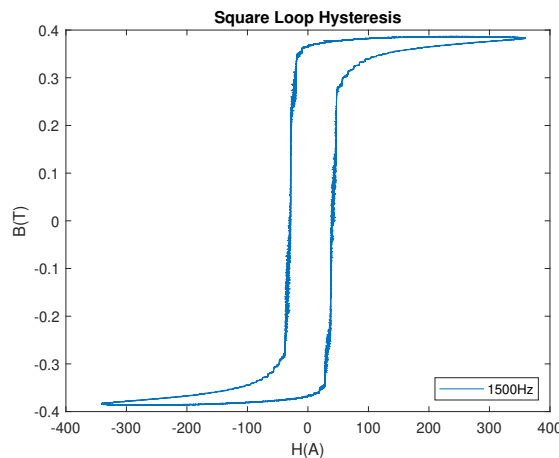


Figure 19: Hysteresis Plot when a Ramp of 1500Hz applied

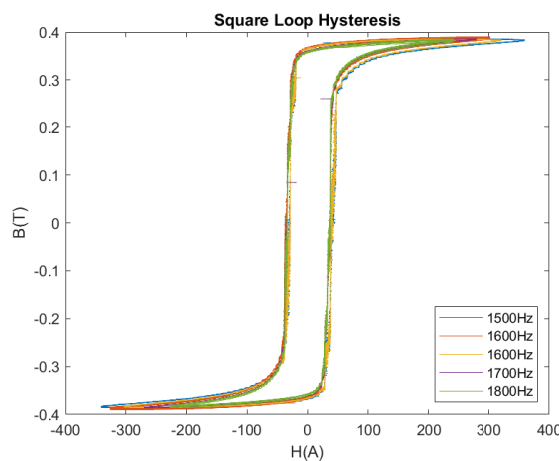


Figure 20: Overlaid plot of Hysteresis at different frequencies

7.2 Negative Inductance

7.2.1 Results Obtained Using Source-Meter-Unit

The source meter is used as a current source to excite the test setup in Figure 7. The test set up was run with sweep of parameters such as the Parallel Resistance, Number of Turns, Amplitude of Current, Frequency of Waveform etc.

The particular situation highlighted here is with **40 turns** and a parallel resistance of **0.2**.

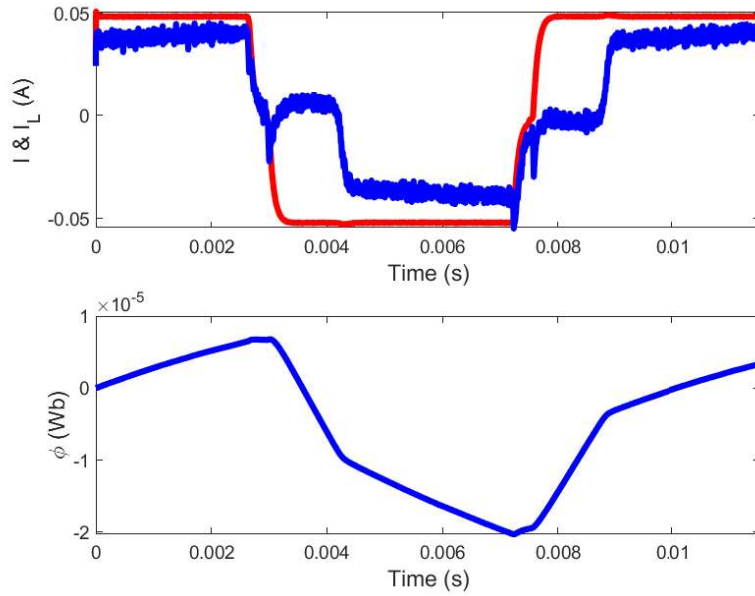


Figure 21: Square Current Waveform Response with SMU(top),Flux in the inductor (Bottom)

7.2.2 Results From the V-I converter

The VI Convertor is used as a current source to excite the test setup in Figure 7. The test set up of again run with a sweep of parameters like Parallel Resistance, Number of Turns,

Amplitude of Current, Frequency of Waveform etc.

The particular situation highlighted here is with **100** turns and Parallel Resistance of 1.2Ω with a current amplitude of 2APP.

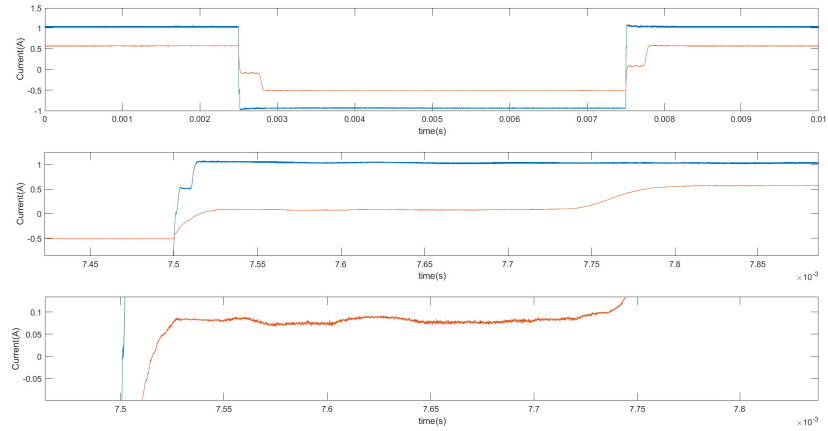


Figure 22: Current Waveforms of Total Current(Blue) and Inductor Current(Orange)

The Flux versus Current plots of the inductor are given here.

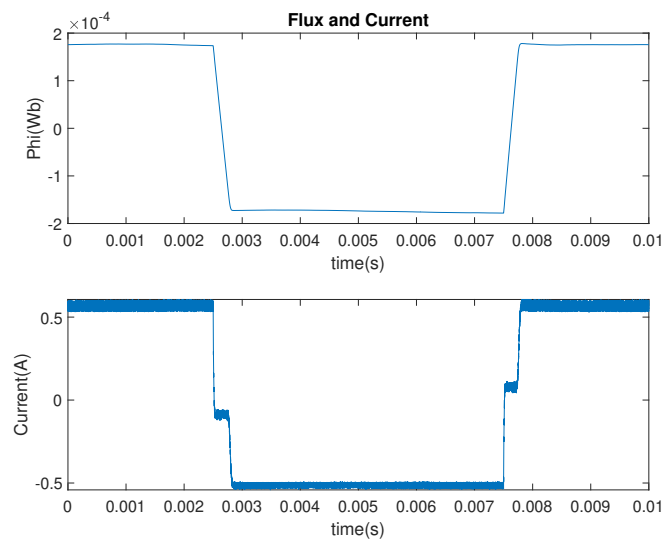


Figure 23: Flux versus Current of Inductor

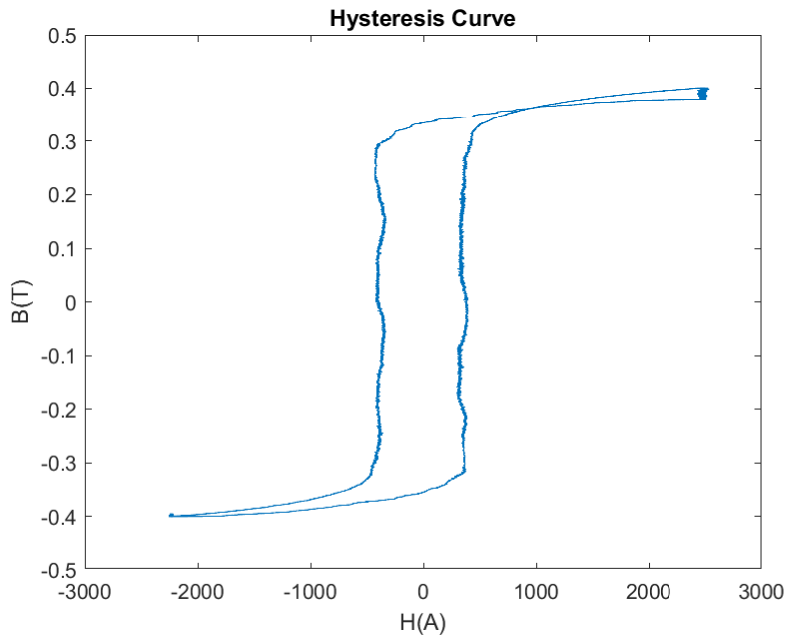


Figure 24: Hysteresis

The particular situation highlighted here is with **100** turns and Parallel Resistance of 1.2Ω with a current amplitude of 1APP.

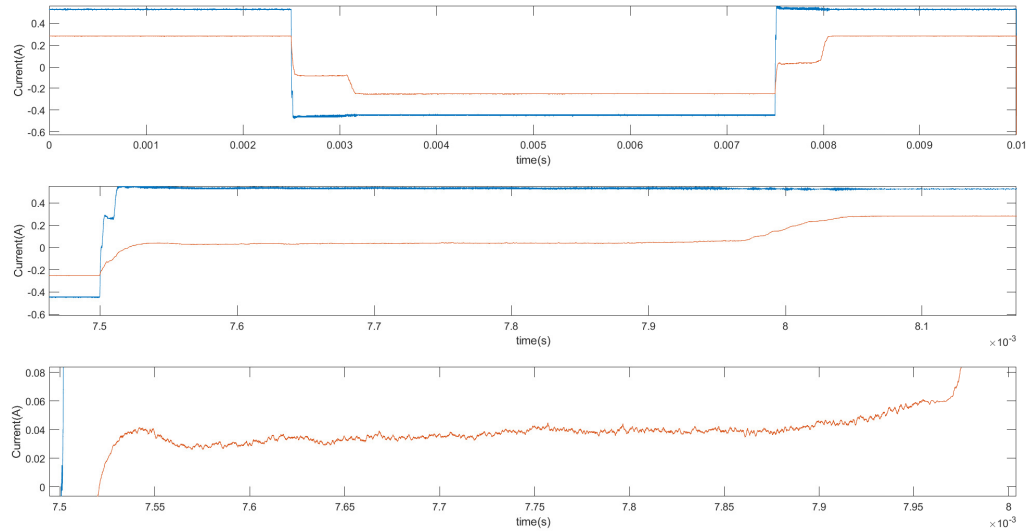


Figure 25: Zoomed Current Waveforms of Total Current(Blue) and Inductor Current(Orange)

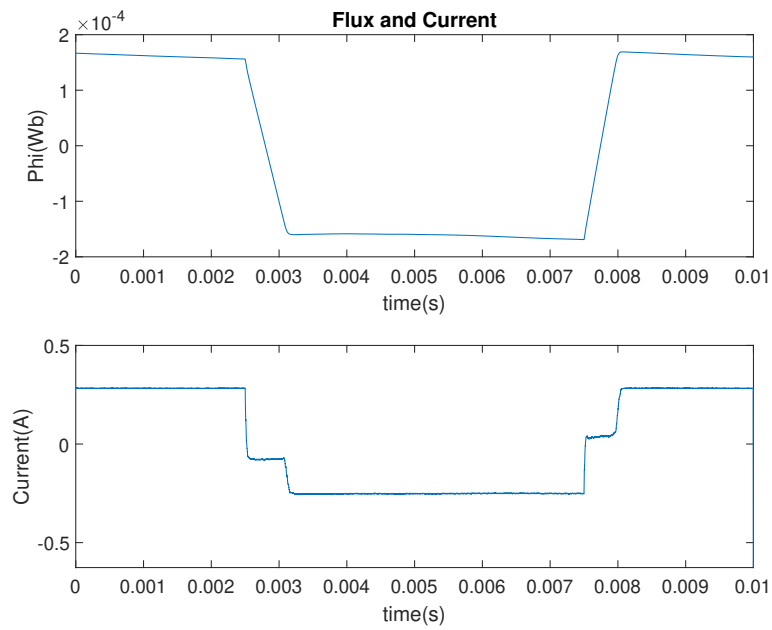


Figure 26: Flux versus Current of Inductor

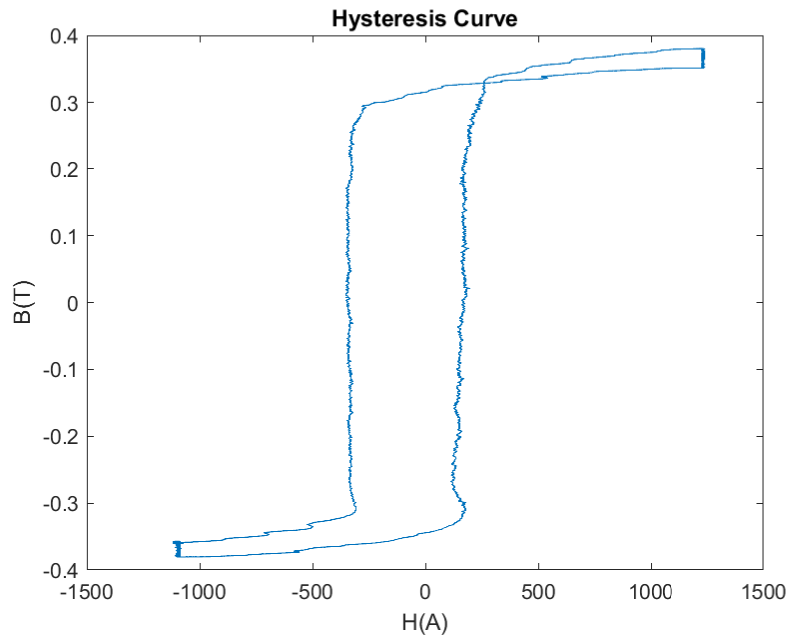


Figure 27: Hysteresis

8 Conclusion

8.1 Comprehending Simulation and Measurement Results

With both the simulation and experimental results in hand, the parallels that can be drawn are the effects as seen in the simulation model are not seen as exaggerated in the experimental result. As seen in the Figures in the Experimental set up, the drop in current is not visible when the current applied is 2APP but the phenomenon seems to manifest when the current applied is 1APP. In the Figure 22, it can be seen that the current response is more-or less flat. Whereas in Figure 25, it can be seen that there is about a 100mA drop in current and this drop is evident in the **pinched hysteresis** which can be seen in the Figure 27 as opposed to the Figure 24 where a regular hysteresis is seen.

8.2 Comparison With the Negative Capacitance Results

This is similar to the negative capacitance results, it can be seen that the current waveforms are similar to the voltage waveforms seen in the ferroelectric capacitors. The Figure 28 shows the similarity of waveforms and the the Figure 29 shows that the core is indeed switching and that is not a measurement artifact.

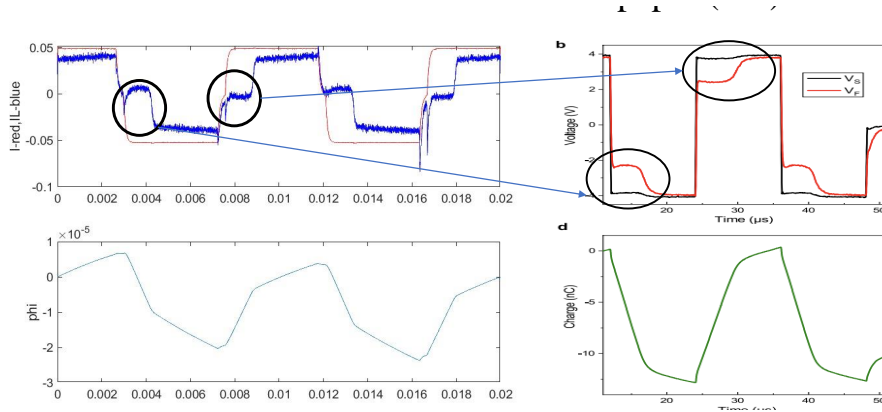


Figure 28: Negative Capacitance Comparison

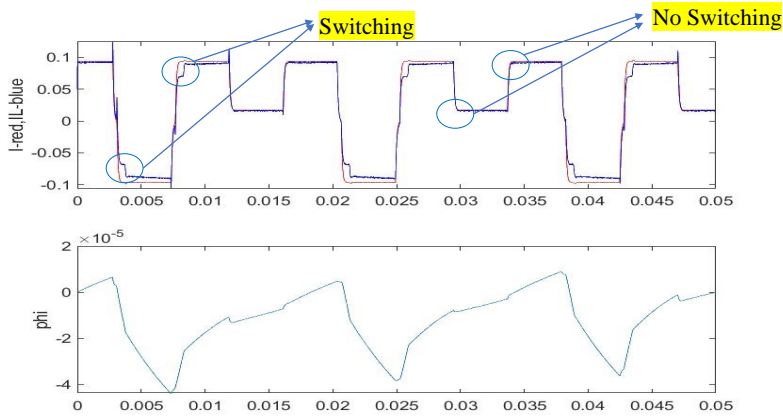


Figure 29: Switching and Non-Switching of the Core

References

- [1] Asif Islam Khan, Korok Chatterjee, Brian Wang, Steven Drapcho, Long You, Claudy Serrao, Saidur Rahman Bakaul, Ramamoorthy Ramesh, and Sayeef Salahuddin. Negative capacitance in a ferroelectric capacitor. *Nature materials*, 14(2):182–186, 2015.
- [2] Suhas Kumar and R. Stanley Williams. Tutorial: Experimental nonlinear dynamical circuit analysis of a ferromagnetic inductor. *IEEE Circuits and Systems Magazine*, 18(2):28–34, 2018.
- [3] Dr. Arvind Ajoy Priyankka G. R. Transient negative inductnce in ferromagnetic material.
- .
- [4] David F. Chan Collin Wells. Ti precision designs: Verified design 5 Technical report, TI, 2013.